Biomedical Signal Processing and Control 14 (2014) 265–271

Contents lists available at ScienceDirect

Biomedical Signal Processing and Control

journal homepage: www.elsevier.com/locate/bspc

Continuous estimation of finger joint angles under different static wrist motions from surface EMG signals

Lizhi Pan, Dingguo Zhang*, Jianwei Liu, Xinjun Sheng, Xiangyang Zhu

State Key Laboratory of Mechanical System and Vibration, School of Mechanical Engineering, Shanghai Jiao Tong University, Shanghai 200240, PR China

ARTICLE INFO

Article history:
Received 13 December 2013
Received in revised form 7 August 2014
Accepted 7 August 2014
Available online 7 September 2014

Keywords:
Electromyography (EMG)
Partial-hand amputees
Switching regime
Angle estimation
Class-wise stationary subspace analysis (cwSSA)
Pattern classification

ABSTRACT

In this paper, a solution is proposed to predict the finger joint angle using electromyography (EMG) towards application for partial-hand amputees with functional wrist. In the experimental paradigm, the subject was instructed to continuously move one finger (middle finger for able-bodied subjects and index finger for partial-hand amputees) up to the maximum angle of flexion and extension while the wrist was conducting seven different wrist motions. A switching regime, including one linear discriminant analysis (LDA) classifier and fourteen state-space models, was proposed to continuously decode finger joint angles. LDA classifier was used to recognize which static wrist motion that the subject was conducting and choose the corresponding two state-space models for decoding joint angles of the finger with two degrees of freedom (DOFs). The average classification error rate (CER) was 6.18%, demonstrating that these seven static wrist motions along with the continuous movement of the finger could be classified. To improve the classification performance, a preprocessing method, class-wise stationary subspace analysis (cwSSA), was firstly adopted to extract the stationary components from original EMG data. Consequently, the average CER was reduced by 1.82% ($p < 0.05$). The state-space model was adopted to estimate the finger joint angle from EMG. The average estimation performance (index R^2) of the two joint angles of the finger across seven static wrist motions achieved 0.843. This result shows that the finger's joint angles can be continuously estimated well while the wrist was conducting different static motions simultaneously. The average accuracy of seven static wrist motions with and without cwSSA and the average estimation performance of the two joint angles of the finger prove that the proposed switching regime is effective for continuous estimation of the finger joint angles under different static wrist motions from EMG.

1. Introduction

Approximately 18,496 people undergo upper-limb amputations each year in the United States, only second to trauma, cancer or peripheral vascular disease [1]. More than 92% of these upper-limb amputees are partial-hand amputees who have amputation level that is distal to the wrist [1,2], while most of the commercial prostheses companies produce the whole-hand prostheses. Although partial-hand prostheses were widely described in historical research, it is not an amputation level on which researchers and clinicians have focused [3]. It is obvious that partial-hand amputees have been ignored for a long time in the fields of prostheses research and manufacturing.

In recent years, two kinds of powered partial-hand prostheses with individually-functioning digits, i.e. ProDigits system (Touch Bionics Inc.) and Vincent finger system (Medical Technics), as shown in Fig. 1, were commercially-available [4]. The control strategies of both systems were still traditional proportional control or on-off switch using surface electromyography (EMG) signals [5,6]. Multi-sensory information, such as force sensitive resistor (FSR), was used in some cases, but those control methods were also very simple. The pattern recognition method has been applied in upper limb amputees for 20 years [7]. However, the acceptance of powered upper limb prostheses based on pattern recognition is still limited, even though the recognition accuracy could be >95% by using the state-of-art technology [8–10]. One main reason is that the pattern recognition based myoelectric control just realizes discrete motions of prosthesis, which is different from the natural and smooth human movements. Users may prefer continuous and intuitive control [11].

It is one of the major challenges in myoelectric control to provide simultaneous and proportional control signals for

* Corresponding author. Tel.: +86 02134206072.
E-mail address: dgzhang@sjtu.edu.cn (D. Zhang).

http://dx.doi.org/10.1016/j.bspc.2014.08.004
1746-8094/

Fig. 1. ProDigits system (Touch Bionics Inc.) and Vincent finger system (Medical Technics).

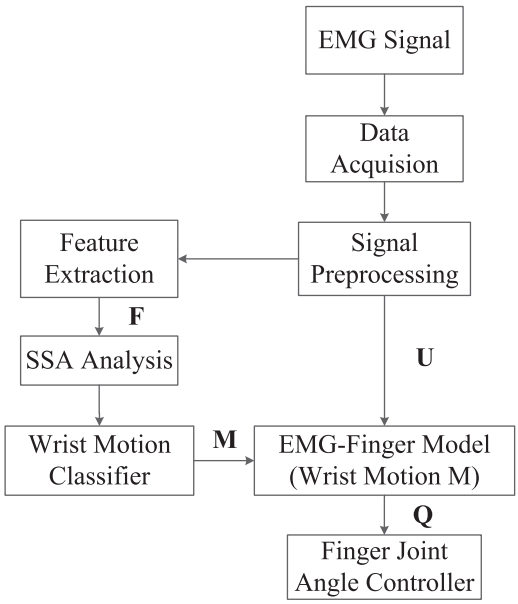

Fig. 2. Block diagram of the proposed switching regime. M is the output of wrist motion classifier, while Q is the finger joint angle.

powered hand prostheses with multiple degrees of freedom (DOFs) [12]. Proportional control has been studied by many researchers for wrist movements. Non-negative matrix factorization algorithm was adopted to simultaneously estimate the wrist torque of three DOFs by Jiang et al. [13]. A mirrored bilateral training strategy was employed to estimate contra-lateral wrist torque using EMG from the ispi-lateral limb by Nielsen et al. [11]. Then, mirrored bilateral training strategy was adopted to simultaneously and proportionally estimate wrist kinematics in uni-lateral trans-radial amputees by Jiang et al. [14]. Meanwhile, continuous estimation of the finger joint angles from EMG signals was studied by several researchers. Artificial neural network (ANN) was widely used in continuous estimation of finger joint angles from EMG signals [15–17]. Hammerstein-Weiner Model was adopted to continuously decode the finger joint angles from EMG signals [18]. We also did some work on continuously decoding finger joint angles from EMG signals using state-space models [19]. However, all previous methods as mentioned above have not taken wrist movements into consideration, merely let the subject hold his/her wrist at neutral position in the experimental paradigm. Consequently, the estimation performances of continuous movements of the finger were relatively feasible, but inapplicable for partial-hand amputees for the reason that finger movements always exist along with wrist movements which would impair the estimation accuracy of finger joint angles. Thus, the impact of static wrist motions on continuous estimation model of finger joint angles was investigated in this study.

A new experimental paradigm was proposed, requiring the subject to move his/her one finger (middle finger for able-bodied subjects and index finger for partial-hand amputees) up to the maximum angle of flexion and extension while his/her wrist was under seven different static motions (neutral position, flexion, extension, radial deviation, ulnar deviation, pronation and supination). A switching regime, including one linear discriminant analysis (LDA) classifier and fourteen state-space models, was proposed to continuously decode the finger joint angles for partial-hand amputees (Fig. 2). LDA classifier was used to classify which static wrist motion that the subject was conducting and choose the corresponding two state-space models for decoding two joint angles of the finger. One state-space model was adopted to estimate one finger joint angle from EMG. Stationary subspace analysis (SSA) was a method to factorize a high-dimensional multivariate time-series into its stationary and non-stationary components [20]. SSA has been widely used to find stationary brain sources in electroencephalograph (EEG) data to improve the pattern recognition accuracy [21,22]. Class-wise analysis has been used in pattern recognition from EMG signals [23]. In order to achieve higher accuracy of classification, class-wise SSA (cwSSA) was firstly adopted to extract stationary components from raw EMG data.

2. Methods

2.1. Subjects

Six able-bodied subjects (five males and one female; aged 23–26) and two partial-hand amputees (one male and one female; aged 56–57) participated in the experiment. Both of the two partial-hand amputees had an index finger amputation of the left hand. This work was approved by the Ethics Committee of Shanghai Jiao Tong University. All subjects participating in the experiment had signed the informed consent and the procedures were in compliance with the Declaration of Helsinki.

2.2. Experimental paradigm

A subject was instructed to be seated in a chair with his/her arm along the body resting on the armrest. Then, the subject was instructed to repeat one-finger movements (middle finger for able-bodied subjects and index finger for partial-hand amputees) from neutral position while holding the rest of fingers in a neutral position. The subject was told to move the finger up to the maximum angle of flexion and extension while holding his/her wrist in the following positions: neutral position, flexion, extension, radial deviation, ulnar deviation, pronation and supination. On each wrist position, the subject was instructed to repeat moving the finger up to the maximum angle of flexion and extension for 50 s. For partial-hand amputees, mirrored bilateral training strategy was adopted [11]. The partial-hand amputees were instructed to perform mirrored bilateral movements as mentioned above. Since the partial-hand amputees had no index finger of the left hand, they were asked to perform phantom index movements of the left hand during mirrored bilateral training process. The contra-lateral joint

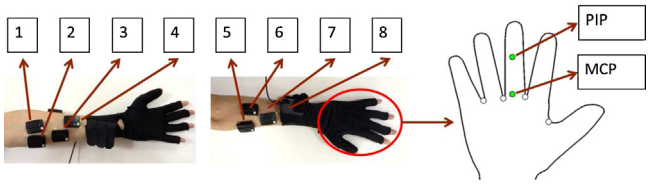

Fig. 3. Able-bodied subjects: surface EMG electrodes were attached on left forearm, and finger joint angles (MCP, PIP) of left middle finger were acquired by 5DT Data Glove 14 Ultra.

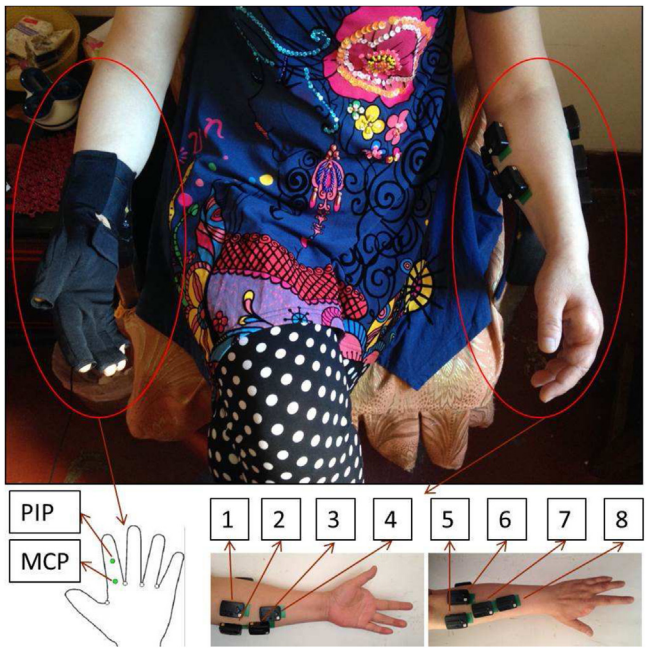

Fig. 4. Partial-hand amputees (the left index finger was lost): surface EMG electrodes were attached on left forearm, and finger joint angles (MCP, PIP) of right index finger were acquired by 5DT Data Glove 14 Ultra.

angles of the index finger could be considered as the joint angles of the amputated finger. In order to avoid muscle fatigue, the subjects had at least 5 min rest between different wrist positions.

2.3. Data acquisition

For surface EMG signal acquisition, a Trigno Wireless System (Delsys Inc., USA) was used. As shown in Fig. 3 and Fig. 4, eight-channel surface EMG signals were recorded from seven muscles related to the finger and wrist movements: 1. Flexor Carpi Radialis, 2. Flexor Carpi Ulnaris, 3. Flexor Digitorum Profundus, 4. Flexor Digitorum Superficialis, 5. Extensor Carpi Radialis, 6. Extensor Carpi Ulnaris, 7. Extensor Digitorum, 8. Extensor Digitorum. Eight wireless noninvasive surface electrodes were placed over the target muscles using medical adhesive tape. The electrodes were wirelessly connected to Trigno Base Station which would be communicating with a computer through USB link. The EMG signals were band-pass filtered (with pass band of 20–450 Hz) and sampled at 2000 Hz by the EMG data acquisition system.

For finger joint angles acquisition, a 5DT Data Glove 14 Ultra (5DT Inc., USA) was used in the experiment. As shown in Fig. 3, the able-bodied subject wore a 5DT Data Glove on the left hand and the angles of the metacarpophalangeal joint (MCP) and the proximal interphalangeal joint (PIP) of the middle finger were measured. Different from the able-bodied subjects, the mirrored bilateral training strategy was used for amputees. As shown in Fig. 4, the partial-hand amputees wore a 5DT Data Glove on the right hand and the MCP and the PIP of the index finger were measured, which were used as the measured angles to identify the estimated angles from EMG acquired on the contra-lateral (left) side. The scaled finger joint angle from the 5DT Data Glove was used.

The Software Development Kits (SDKs) of Trigno Wireless System and 5DT Data Glove 14 Ultra were used to develop a *c*♯ program that can simultaneously sample EMG signals and finger joint angles at 2000 Hz and write the data to a text file.

2.4. Wrist motion classification

2.4.1. Feature extraction

Feature extraction is a necessary step for pattern recognition. As the effectiveness of time-domain (TD) feature set had been repeatedly demonstrated in previous studies on EMG pattern recognition [7,24,25], the TD features were adopted in this study. TD features were originally proposed by Hudgins et al. [7], where continuous EMG signals were segmented into multiple analysis windows and TD features were extracted from each analysis window. The EMG signal from one channel can be represented as a finite time series $(x_1, x_2, \ldots, x_N)$ where N is the number of samples in an analysis window. The TD feature set for this time series includes four statistics, which are:

(1) Mean absolute value (MAV)

$$\mathrm{MAV} = \frac{1}{N}\sum_{i=1}^{N}|x_i| \tag{1}$$

(2) Number of zero crossings (ZC)

$$\mathrm{ZC} = \sum_{i=2}^{N}\mathrm{sgn}(-x_i x_{i-1}) \tag{2}$$

(3) Waveform length (WL)

$$\mathrm{WL} = \frac{1}{N-1}\sum_{i=2}^{N}|x_i - x_{i-1}| \tag{3}$$

(4) Number of slope changes (SSC)

$$\mathrm{SSC} = \sum_{i=3}^{N}\mathrm{sgn}[-(x_i - x_{i-1})(x_{i-1} - x_{i-2})] \tag{4}$$

where $\mathrm{sgn}(x)$ is a sign function, which is defined as

$$\mathrm{sgn}(x) = \begin{cases} 1 & \text{if } x > 0 \\ 0 & \textit{otherwise}. \end{cases} \tag{5}$$

The analysis window was set to 200 ms and the increment of analysis window, which was the interval between two adjacent windows, was set to 50 ms. A feature set was computed on each of the eight channels, and then concatenated to form a 32-dimensional feature vector. Therefore, 7000 feature samples were taken for each subject in all.

2.4.2. Classification

As a simple classifier which is fast to train, LDA classifier has been widely used in EMG signals pattern recognition [26,27]. It has been presented in previous studies that LDA classifier can have the same performance as more complex and potentially more powerful classifiers [28]. Hence, LDA classifier was adopted to identify the seven static wrist motions. One half of the data were used as a training set to train LDA classifier, and the other half were used as a testing set to evaluate the classification performance.

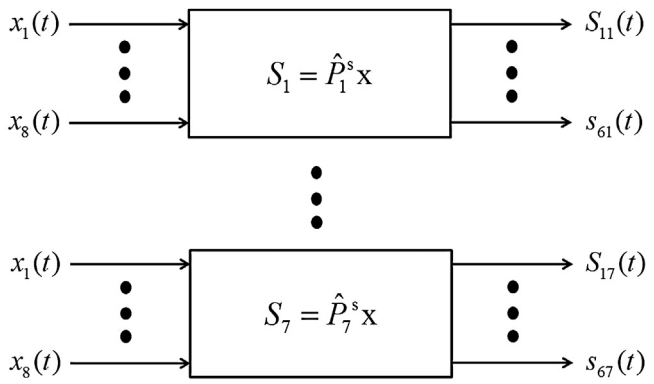

Fig. 5. Block diagram indicating cwSSA tuning preprocessing block.

2.5. Finding stationary sources in EMG data

2.5.1. Class-wise stationary subspace analysis

SSA was originally proposed by Paul et al. [20], as a method to factorize a multivariate time series into its stationary and non-stationary components. Even though widely used to find stationary brain sources in EEG data [21,22], SSA has never been used in EMG data analysis. In SSA method, there is a basic assumption that the acquired signal $x(t)$ is a linear superposition of stationary sources (s-sources) $s^s(t)$ and non-stationary sources (n-sources) $s^n(t)$

$$x(t) = As(t) = [\, A^s \quad A^n \,] \begin{bmatrix} s^s(t) \\ s^n(t) \end{bmatrix} \tag{6}$$

and A is an invertible matrix. Finding a linear transformation $\hat{A}^{-1}$ that separates the s-sources from n-sources is the goal of SSA method. $\hat{A}^{-1}$ was defined as:

$$\hat{A}^{-1} = \begin{bmatrix} \hat{P}^s \\ \hat{P}^n \end{bmatrix}. \tag{7}$$

However, the statistical properties of the EMG data are expected to change with the class. SSA is limited when applied to multi-class data for the reason that different classes would be considered as non-stationary components of the signal and thus removed by SSA. To avoid this, class-wise SSA (cwSSA) was adopted. Class-wise means that the separate transformation matrices $\hat{A}_1^{-1}, \hat{A}_2^{-1}, \ldots, \hat{A}_C^{-1}$ were found for each class. Fig. 5 shows that the cwSSA method is available to increase the dimensionality of the input by a factor of C, where C is the total number of classes, which is seven here.

We set the dimension of stationary subspace to be six and the epoch to be the same as the analysis window.

2.5.2. Quantification of feature space

Two metrics, i.e. mean semi-principal axis (MSA) and separability index (SI), were used to quantify the overall pattern characteristics of EMG signals feature space [29].

The MSA was defined to measure hyperellipsoid size, as the geometric mean of the semi-principal axes of the hyperellipsoids:

$$\mathrm{MSA} = \frac{1}{C}\sum_{j=1}^{C}\left(\left(\prod_{k=1}^{nf} a_{jk}\right)^{1/nf}\right) \tag{8}$$

where C is the number of classes, nf is the dimension of the feature vector and a_{jk} is semi-principal axes length corresponding to the kth principal component of class j. In general, the lower MSA indicates the smaller intra-class dispersion. The lower MSA could be caused by the reduction of variability in EMG data for the same motion class.

The SI was defined to measure inter-class distances, as mean value of one-half Mahalanobis distance from the centroid of the ellipsoid of class j (μ_{Tj}) to the centroid of the ellipsoid of the nearest class i (μ_{Ti}) across the C classes:

$$\mathrm{SI} = \frac{1}{C}\sum_{j=1}^{C}\left(\min_{i\neq j}\frac{1}{2}\sqrt{(\mu_{Ti}-\mu_{Tj})^T S_{Tj}^{-1}(\mu_{Ti}-\mu_{Tj})}\right) \tag{9}$$

where S_{Tj} is the covariance of data for class j.

These two metrics were adopted to characterize the variations in EMG feature space with and without cwSSA.

2.6. Estimation of finger joint angles from EMG

2.6.1. Data preprocessing

The EMG signals were full-waved rectified and low-pass filtered (2nd order zero-lag Butterworth digital filter and cut-off frequency 10 Hz) to obtain the muscle activity envelopes. The finger joint angles were low-pass filtered (2nd order zero-lag Butterworth digital filter, cut-off frequency 10 Hz) as well. Then, the filtered EMG signals and the angle data were normalized. The MAV feature was extracted using the same analysis window and the same increment as those specified in Section 2.4.1.

2.6.2. State-space model

In our previous study, the state-space model method has been used for continuous estimation of 10-DOF finger joint angles from EMG signals [19]. In this work, one state-space model was also used to estimate one finger joint angle from EMG signals.

$$\begin{aligned} x(k+1) &= Gx(k) + Bu(k) \\ y(k) &= Dx(k) \end{aligned} \tag{10}$$

where x is the hidden state vector, y is the finger joint angle, u is the muscle activations, G is the system matrix representing the dynamic behavior of the hidden state vector x, B is the matrix imaging the EMG signal u to the state vector x, and D is the matrix representing the relationship between the finger joint angle y and the state vector x. We used different state-space models for different finger joint angles to obtain a better estimation performance for each DOF. Therefore, fourteen state-space models were used to estimate the MCP and PIP of the finger under seven different static wrist motions. Each state-space model used EMG signals as input and one of the finger joint angles as output. The state-space models were identified with "N4SID" algorithm [30], which is a subspace method for estimating the parameters of the state-space model. It should be indicated that the state-space models identified for either able-bodied subjects or partial-hand amputees were using the same method.

For all state-space models, the first half data were used for identification of the model parameters and the second half were used for estimation. In order to evaluate the estimation performance of the state-space model in each finger joint angle, the coefficient of determination R^2 was used [31]. The index R^2 is defined as follows:

$$R^2 = 1 - \frac{\sum_{t=0}^{N}(\widehat{f(\mathrm{t})} - f(\mathrm{t}))^2}{\sum_{t=0}^{N}(f(\mathrm{t}) - \bar{f(\mathrm{t})})^2} \tag{11}$$

where N is the number of data samples, $f(\mathrm{t})$ is the finger joint angle function, $\widehat{f(\mathrm{t})}$ is the corresponding estimated finger joint angle from the state-space model, and $\bar{f(\mathrm{t})}$ is the temporal average of $f(\mathrm{t})$.

The time cost was estimated in a 2.4 GHz intel Core i5 computer running MATLAB. The time cost of identifying one point of joint angle was 53.011 ms.

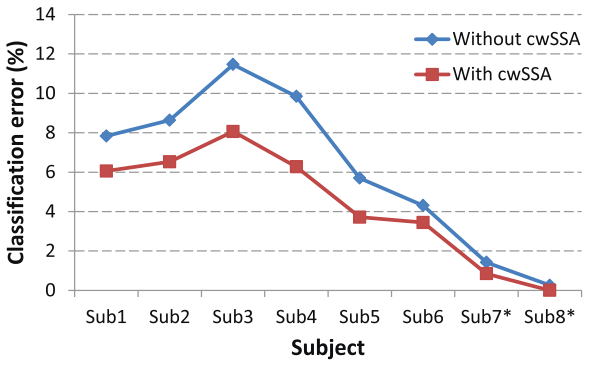

Fig. 6. Classification error rates with and without cwSSA. The star sign * indicates the partial-hand amputees.

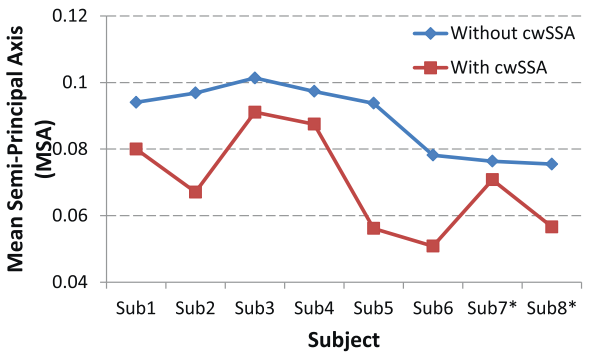

Fig. 7. MSA of the feature vector with and without cwSSA. The star sign * indicates the partial-hand amputees.

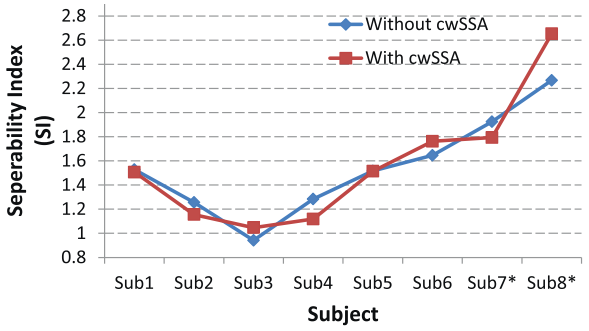

Fig. 8. SI of the feature vector with and without cwSSA. The star sign * indicates the partial-hand amputees.

3. Results

3.1. Classification error rate of wrist motions

We compare the results in two cases that are represented by "with cwSSA" and "without cwSSA". In case of "with cwSSA", the raw EMG data are processed by cwSSA method to extract stationary components. In case of "without cwSSA", the raw EMG data are not processed by cwSSA.

As shown in Fig. 6, classification error rate (CER) of the wrist motions without cwSSA along with the continuous movement of the finger can be less than 12% on all subjects and the mean value is 6.18%. The result shows that these seven static wrist motions can be classified by a LDA classifier even if the finger was continuously moving during each static wrist motion.

The average CER of each static wrist motion across eight subjects without cwSSA is illustrated in Table 1. The result shows that the CER of each wrist motion can be less than 10%, proving that each static wrist motion can be classified while the finger was moving.

As shown in Fig. 6, with cwSSA, CER of wrist motions along with continuous movement of the finger can be decreased to less than 8% on each subject and the mean value can be decreased to 4.36%. The statistical test shows that the improvement of cwSSA in CER is significant ($p < 0.05$).

As shown in Table 1, with cwSSA, average error rate of each static wrist motion across eight subjects can be less than 5%, which is a relatively good result as each static wrist motion was along with continuous movement of the finger. It is indicated by comparison of average CER of each static wrist motion with and without cwSSA that cwSSA is available for significant improvement of classification performance of each static wrist motion ($p < 0.05$).

3.2. Variations in EMG feature space

In order to better understand whether class-wise analysis or SSA is the main cause for decrease of wrist motion CER, MSA and SI of each subject with and without cwSSA are compared in Fig. 7 and Fig. 8.

As cwSSA method is available to increase the dimensionality of input, prior to computation of MSA and SI, the Fisher linear discriminant (FLD) [32] was adopted to reduce the dimension of feature vectors with and without cwSSA to the same level of $C - 1$, where C is the number of classes.

Fig. 7 demonstrates that MSA of EMG feature vectors are significantly decreasing with cwSSA ($p < 0.05$), indicating that intra-class dispersion become smaller after the process of cwSSA. As shown in Fig. 8, there is no significant variation between SIs of EMG feature vectors with and without cwSSA ($p > 0.05$), demonstrating that inter-class distance has no significant change after the process of cwSSA. Therefore, the results show that the significant decrease of MSA of EMG feature vectors is the main cause for the decrease of wrist motion CER. Since the decrease of the MSA is mainly caused by SSA, as we will discuss in the relevant part, the results also show that SSA is the main cause for the drop of wrist motion CER.

Table 1
Classification error rate of each static wrist motion.

Classification error (%)	Without cwSSA	With cwSSA	Error rate reduction
Neutral position	5.80	4.48	1.32
Flexion	5.80	4.78	1.02
Extension	6.05	4.48	1.57
Radial deviation	4.83	4.20	0.63
Ulnar deviation	9.02	4.86	4.17
Pronation	5.16	4.27	0.89
Supination	6.60	3.48	3.13
Mean	6.18	4.36	1.82

3.3. Estimation accuracy of finger joint angles

The average index R^2 for each MCP and PIP joints of the finger under seven static wrist motions are illustrated in Fig. 9. The average estimation performance (index R^2) of two joint angles of the finger under different static wrist motions can be achieved as follows: 0.887 (neutral position), 0.838 (flexion), 0.849 (extension), 0.831 (radial deviation), 0.820 (ulnar deviation), 0.855 (pronation) and 0.820 (supination). The grand mean value of the index R^2 across these seven groups is 0.843. As there is no previous work on continuous estimation of the finger joint angles while wrist is under seven different static motions, the results are also pretty good compared with the estimation performance of finger joint angles while the wrist is only at neutral position in previous studies

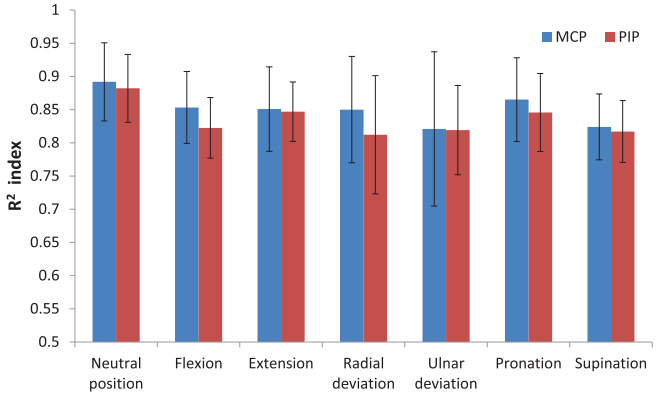

Fig. 9. Average R^2 index for each MCP and PIP joints of the finger (middle finger for able-bodied subject and index finger for partial-hand amputee) under seven static wrist motions. Error bars represent the standard deviation.

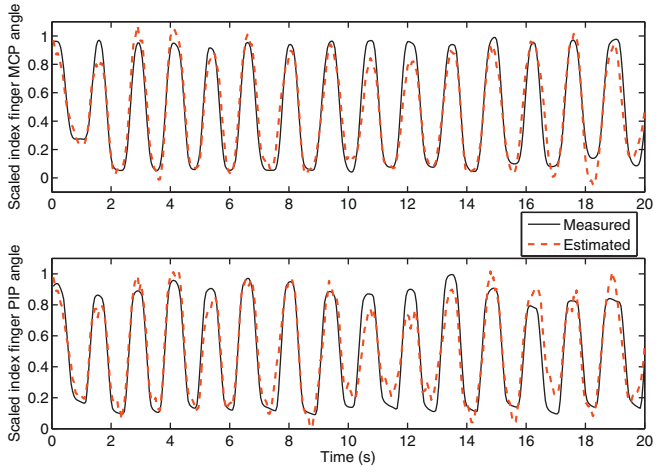

Fig. 10. Measured and estimated MCP and PIP joint angles of the index finger while the wrist is conducting pronation for the partial-hand amputee (Sub8*). In this example, the index R^2 are 0.899 (MCP) and 0.850 (PIP).

[15–17,19]. Fig. 10 shows the representative results from a partial-hand amputee (Sub8*).

4. Discussion and conclusion

The average CER of seven static wrist motions across eight subjects can be as low as 6.18% without cwSSA, thereby illustrating that seven static wrist motions along with continuous movement of the finger can be classified by a LDA classifier. Since the static wrist motions are accompanied with the continuous movement of the finger, the CER is not as low as that of static wrist motions without finger movements. However, this result is relatively good in the proposed experimental paradigm, in which the subject moved the finger up to the maximum angle of flexion and extension while his/her wrist was under seven different static motions, and originally verify the separability of static wrist motions along with the continuous movement of the finger.

Further, the average CER of the seven static wrist motions across eight subjects significantly decreases from 6.18% without cwSSA to 4.36% with cwSSA, as shown in Fig. 6 and Table 1. In this study, the EMG signals acquired can be regarded as a linear superposition of EMG signal generated by static wrist motions and EMG signal generated by continuous movement of the finger. The EMG signals generated by the static wrist motion can be considered as the stationary source. The EMG signals generated by such continuous movement can be considered as non-stationary source. Therefore, SSA is suitable to improve the classification performance of wrist motions by extracting stationary source from EMG signals for classification. The effect of SSA is demonstrated by the decrease of the intra-class dispersion, which means that the feature vector of each static wrist motion is more stable. As MSA of such feature vector represents intra-class dispersion, the decrease of the MSA is mainly caused by SSA. The effect of class-wise analysis is demonstrated by the increase of the inter-class distance, which means that the feature vector of each static wrist motion is more separable. As SI of such feature vector represents inter-class distance, the increase of the SI is mainly caused by class-wise analysis. As shown in Fig. 7 and Fig. 8, MSA of feature vectors is significantly decreased with cwSSA ($p < 0.05$) while there is no obvious variation between SIs of EMG feature vectors with and without cwSSA ($p > 0.05$). In our opinion, SSA is the main cause for the decrease of wrist motion CER.

Fig. 6 demonstrates that the CERs without cwSSA of the partial-hand amputees were lower than the able-bodied subjects. This phenomenon can be explained by that the EMG signals generated by continuous movement of the amputated finger were weaker than the EMG signals generated by continuous movement of the intact finger. The EMG signals generated by continuous movement of the finger can be considered as non-stationary source. Therefore, the weaker the non-stationary sources were, the lower the CERs were. Even if the CERs without cwSSA of the partial-hand amputees were pretty low (less than 2%), cwSSA can further reduce the CERs.

Fig. 7 shows that Sub7* has a relatively smaller reduction of MSA after the process of cwSSA, compared with the other subjects. This phenomenon is attributed to two reasons: (1) the ceiling effect that causes the reduction of MSA on Sub7* is smaller than that on the other subjects, since the MSA without cwSSA of Sub7* is already at a pretty low level; (2) individual difference makes that the cwSSA has less effect on Sub7*.

At last, the result that the average estimation performance (index R^2) of two joint angles of the finger under different static wrist motions is higher than 0.8 proves that finger joint angle can be continuously decoded by a state-space model while the wrist is under static motion.

The CERs of static wrist motions with and without cwSSA and average estimation performance of two joint angles of the finger show that the proposed switching regime, including one LDA classifier and fourteen state-space models, is available for continuous estimation of the finger joint angles under different static wrist motions from surface EMG signals for partial-hand amputees.

Acknowledgments

We hereby express our great gratitude to all subjects participating in this experiment. This work was supported by the National Basic Research Program (973 Program) of China (Grant No. 2011CB013305), the Science and Technology Commission of Shanghai Municipality (Grant No. 11JC1406000, 13430721600), and the State Key Laboratory of Mechanical System and Vibration (Grant No. MSVZD201204).

References

[1] T.R. Dillingham, L.E. Pezzin, E.J. MacKenzie, Limb amputation and limb deficiency: epidemiology and recent trends in the United States, South. Med. J. 95 (8) (2002) 875–883.
[2] K. Ziegler-Graham, E.J. MacKenzie, P.L. Ephraim, T.G. Travison, R. Brookmeyer, Estimating the prevalence of limb loss in the United States: 2005 to 2050, Arch. Phys. Med. Rehabil. 89 (3) (2008) 422–429.
[3] C. Lake, Experience with electric prostheses for the partial hand presentation: an eight-year retrospective, J. Prosthet. Orthot. 21 (2) (2009) 125–130.
[4] J. Uellendahl, E. Uellendahl, Experience fitting partial hand prostheses using prodigits, in: University of New Brunswick MyoElectric Controls/Powered Prosthetics Symposium, Fredericton, New Brunswick, Canada, 2008.

[5] A.H. Bottomley, Myoelectric control of powered prostheses, J. Bone Joint Surg. Br. 47-B (3) (1965) 411–415.
[6] D.S. Childress, A myoelectric three-state controller using rate sensitivity, in: Proceedings of 8th ICMBE, Chicago, IL, 1969, pp. 4–5.
[7] B. Hudgins, P. Parker, R. Scott, A new strategy for multifunction myoelectric control, IEEE Trans. Biomed. Eng. 40 (1) (1993) 82–94.
[8] X. Chen, D. Zhang, X. Zhu, Application of a self-enhancing classification method to electromyography pattern recognition for multifunctional prosthesis control, J. Neuroeng. Rehabil. 10 (1) (2013) 44.
[9] Z. Ju, G. Ouyang, M. Wilamowska-Korsak, H. Liu, Surface EMG based hand manipulation identification via nonlinear feature extraction and classification, IEEE Sens. J. 13 (9) (2013) 3302–3311.
[10] G. Ouyang, X. Zhu, Z. Ju, H. Liu, Dynamical characteristics of surface EMG signals of hand grasps via recurrence plot, IEEE J. Biomed. Health Inform. 18 (2014) 257–265.
[11] J. Nielsen, S. Holmgaard, N. Jiang, K. Englehart, D. Farina, P. Parker, Simultaneous and proportional force estimation for multifunction myoelectric prostheses using mirrored bilateral training, IEEE Trans. Biomed. Eng. 58 (3) (2011) 681–688.
[12] A. Fougner, O. Stavdahl, P. Kyberd, Y. Losier, P. Parker, Control of upper limb prostheses: terminology and proportional myoelectric control – a review, IEEE Trans. Neural Syst. Rehabil. Eng. 20 (5) (2012) 663–677.
[13] N. Jiang, K. Englehart, P. Parker, Extracting simultaneous and proportional neural control information for multiple-DOF prostheses from the surface electromyographic signal, IEEE Trans. Biomed. Eng. 56 (4) (2009) 1070–1080.
[14] N. Jiang, J.L. Vest-Nielsen, S. Muceli, D. Farina, et al., EMG-based simultaneous and proportional estimation of wrist/hand kinematics in uni-lateral transradial amputees, J. Neuroeng. Rehabil. 9 (1) (2012) 42.
[15] R.J. Smith, F. Tenore, D. Huberdeau, R. Etienne-Cummings, N.V. Thakor, Continuous decoding of finger position from surface EMG signals for the control of powered prostheses, in: 30th Annual International Conference of the IEEE, Engineering in Medicine and Biology Society, 2008 (EMBS 2008), IEEE, 2008, pp. 197–200.
[16] M. Hioki, H. Kawasaki, Estimation of finger joint angles from sEMG using a recurrent neural network with time-delayed input vectors, in: IEEE International Conference on Rehabilitation Robotics, 2009 (ICORR 2009), IEEE, 2009, pp. 289–294.
[17] J. Ngeo, T. Tamei, T. Shibata, Continuous estimation of finger joint angles using muscle activation inputs from surface EMG signals, in: 2012 Annual International Conference of the IEEE, Engineering in Medicine and Biology Society (EMBC), IEEE, 2012, pp. 2756–2759.
[18] P. Kumar, A. Sebastian, C. Potluri, A. Ilyas, M. Anugolu, A. Urfer, M.P. Schoen, Adaptive finger angle estimation from sEMG data with multiple linear and nonlinear model data fusion, in: The 10th World Scientific and Engineering Academy and Society (WSEAS) International Conference on Dynamical Systems and Control, Iasi, Romania, 2011.
[19] L. Pan, X. Sheng, D. Zhang, X. Zhu, Simultaneous and proportional estimation of finger joint angles from surface EMG signals during mirrored bilateral movements, in: Intelligent Robotics and Applications, Springer, Berlin, Heidelberg, 2013, pp. 493–499.
[20] P. von Bünau, F.C. Meinecke, F.C. Király, K.-R. Müller, Finding stationary subspaces in multivariate time series, Phys. Rev. Lett. 103 (21) (2009) 214101.
[21] P. von Bünau, F.C. Meinecke, S. Scholler, K.-R. Müller, Finding stationary brain sources in EEG data, in: 2010 Annual International Conference of the IEEE, Engineering in Medicine and Biology Society (EMBC), IEEE, 2010, pp. 2810–2813.
[22] W. Samek, M. Kawanabe, C. Vidaurre, Group-wise stationary subspace analysis – a novel method for studying non-stationarities, in: Proc. 5th Int. Brain-Computer Interface Conf., 2011, pp. 16–20.
[23] L.J. Hargrove, G. Li, K.B. Englehart, B.S. Hudgins, Principal components analysis preprocessing for improved classification accuracies in pattern-recognition-based myoelectric control, IEEE Trans. Biomed. Eng. 56 (5) (2009) 1407–1414.
[24] H. Huang, P. Zhou, G. Li, T.A. Kuiken, An analysis of EMG electrode configuration for targeted muscle reinnervation based neural machine interface, IEEE Trans. Neural Syst. Rehabil. Eng. 16 (1) (2008) 37–45.
[25] P. Zhou, M.M. Lowery, K.B. Englehart, H. Huang, G. Li, L. Hargrove, J.P. Dewald, T.A. Kuiken, Decoding a new neural-machine interface for control of artificial limbs, J. Neurophysiol. 98 (5) (2007) 2974–2982.
[26] X. Chen, X. Zhu, D. Zhang, Use of the discriminant Fourier-derived cepstrum with feature-level post-processing for surface electromyographic signal classification, Physiol. Meas. 30 (12) (2009) 1399.
[27] K. Englehart, B. Hudgins, A robust, real-time control scheme for multifunction myoelectric control, IEEE Trans. Biomed. Eng. 50 (7) (2003) 848–854.
[28] K. Englehart, B. Hudgins, P.A. Parker, M. Stevenson, Classification of the myoelectric signal using time-frequency based representations, Med. Eng. Phys. 21 (6) (1999) 431–438.
[29] N.E. Bunderson, T.A. Kuiken, Quantification of feature space changes with experience during electromyogram pattern recognition control, IEEE Trans. Neural Syst. Rehabil. Eng. 20 (3) (2012) 239–246.
[30] L. Ljung, System Identification, Wiley Online Library, 1999.
[31] N.R. Draper, H. Smith, E. Pownell, Applied Regression Analysis, vol. 3, Wiley, New York, 1966.
[32] R.O. Duda, P.E. Hart, et al., Pattern Classification and Scene Analysis, vol. 3, Wiley, New York, 1973.